First Principles Calculation of Water pK_a Using the Newly Developed SCAN Functional

Ruiyu Wang[1,2], Vincenzo Carnevale[3,4], Michael L. Klein[1,2,3] and Eric Borguet[1,2*]*

[1]Department of Chemistry, Temple University, Philadelphia, Pennsylvania 19122, United States

[2] Center for Complex Materials from First Principles (CCM), Temple University, 1925 North 12th Street, Philadelphia, Pennsylvania 19122, United States

[3]Institute for Computational Molecular Science, Temple University, Philadelphia, Pennsylvania 19122, United States

[4]Department of Biology, Temple University, Philadelphia, Pennsylvania 19122, United States

ABSTRACT Acid/base chemistry is an intriguing topic that still constitutes a challenge for computational chemistry. While estimating the acid dissociation constant (or pK_a) could shed light on many chemistry processes, especially in the fields of biochemistry and geochemistry, evaluating the relative stability between protonated and non-protonated species is often very difficult. Indeed, a prerequisite for calculating the pK_a of any molecule is an accurate description of the energetics of water dissociation. Here, we applied constrained molecular dynamics simulations, a non-canonical sampling technique, to investigate the water deprotonation process by selecting the OH distance as the reaction coordinate. The calculation is based on density functional theory and the newly developed SCAN functional, which has shown excellent performance in describing water structure. This first benchmark of SCAN on a chemical

reaction shows that this functional accurately models the energetics of proton transfer reactions in an aqueous environment. After taking Coulomb long-range corrections and nuclear quantum effects into account, the estimated water pK_a is only 1.0 pK_a unit different from the target experimental value. Our results show that the combination of SCAN and constrained MD successfully reproduces the chemistry of water and constitutes a good framework for calculating the free energy of chemical reactions of interest.

TOC GRAPHICS

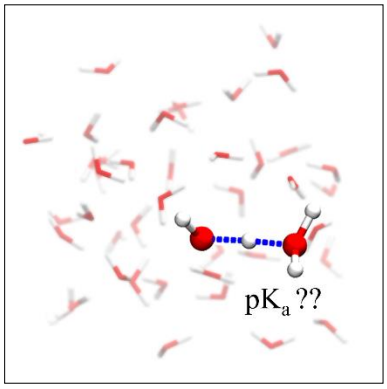

KEYWORDS. Water autoionization, proton transfer, free energy, constrained molecular dynamics, aqueous solution.

Acid/base chemistry is an intriguing topic and draws extensive attention from both experimental and computational chemistry research[1] because of its great impact on catalysis[2], drug design[3] and other related fields. One area that requires accurate predictions of acidity, or pK_a (the acid dissociation constant), is that of mineral oxide surfaces, which are frequently covered with hydroxyl (M-OH) groups; these form crucial hydrogen bonds[4] and their protonation

states affect the structure and dynamics of interfacial water or solutes. Besides the pK_a of minerals, biochemists are interested in the pK_a of amino acids due to the functional consequences of protonation/deprotonation events. For instance, the protonation and deprotonation of histidine is a key component in the gating of the M2 channel of the influenza A virus.[5-6] The pK_a of histidine in bulk water[7-8] and in the His-Trp motif on the M2 protein[9] have been previously analyzed and found to be in qualitative agreement with experiments.

Together with experimental measurements, ab initio molecular dynamics (AIMD) simulations can be used to determine the pK_a. The weak acid dissociation is a rare event on the timescales sampled by typical molecular simulations; therefore, non-canonical sampling techniques are essential to calculate the free energy of the OH bond breaking. The latter can be then easily connected to pK_a, the macroscopic observable that characterizes acidity. For example, Leung el al. and Sulpizi et al. pointed to a bimodal acidity model of amorphous silica/water interfaces, which is in agreement with experimental SHG measurements[10-11]. Recently, the free energy perturbation (FEP) method[12] has been used to study how the quartz/water interface affects the pK_a of an interfacial organic acid molecule, an issue not easily addressable by experiments.[13]

While the FEP method is a mature approach for predicting the pK_a, it can only provide the free energy difference between the initial and final states, neglecting the reaction path, which, by contrast, can be obtained by calculating the potential of mean force (PMF) as a function of appropriately chosen reaction coordinates. Multiple-dimension PMF surfaces have already been used to study weak acid dissociation.[14]

The Helmholtz free energy for the deprotonation can be obtained from the PMF[8]:

$$K_c^{-1} = c_0 \int_0^{R_c} e^{-\beta w(r)} 4\pi r^2 dr \quad (1)$$

$$\mathrm{p}K_a = -logK_c \quad (2)$$

where K_c is the acid dissociation constant, c_0 is the standard concentration, R_c is the distance cutoff for the integral and w(r) is the PMF. This method is approximate in that it neglects zero point energy and tunneling effects, which have been shown to contribute significantly to the pK_a.[8] Moreover, equation (1) assumes that the absolute value of the free energy, w(r), is known for all r values between 0 and R_c (the reference state being when H* and its conjugate base are at infinite separation). This implies that the potential of mean force ought to be calculated from r=0 up to any distance at which w(r) is still significantly different from zero. This constraint results in a severe limitation, given the long-range nature of the interaction between the reactants (hydronium and hydroxide ions) and the limited system size of a typical AIMD simulation. A commonly adopted strategy to mitigate this problem is to focus on the pK_a of the species of interest relative to water[8]:

$$\frac{K_c}{K_w} = \frac{\int_0^{R_c} e^{-\beta w_{water}(r)} r^2 dr}{\int_0^{R_c} e^{-\beta w_{acid}(r)} r^2 dr} \qquad (3),$$

where, K_w is the water ionization constant, 10^{-14}. Despite these challenges, in this paper we attempt to estimate the absolute pK_a of water. To this end, we model the long-range part of the potential of mean force as a screened Coulombic interaction between the hydroxide and the hydronium ions.

Most of the AIMD studies of OH bond breaking have been based on a density functional theory level, given the acceptable compromise between accuracy and computational cost that this approach provides. However, widely used GGA functionals, such as BLYP and PBE predict an over-structured water: hydrogen bonds are stronger and water-water distances are shorter than the experimentally derived values.[15] The dynamics of water are not satisfactory either, diffusion coefficients of proton or hydroxide ion predicted by DFT-MD are not in agreement with experiments.[16] The hybrid functional PBE0 with the Tkatchenko−Scheffler van der Waals

(VDW) corrections predicts reasonably accurate diffusion coefficients of H_3O^+ and OH^-, but its large computational cost makes it unsuitable for large-scale MD simulations.[16] The recently developed meta-GGA functional, strongly constrained and appropriately normed (SCAN)[17], shows good performance in calculating covalent and non-covalent interactions of many systems.[18] MD simulations of bulk water using SCAN successfully predicted the structure[15], dynamics[19] and the IR spectra[20] of bulk water, as well as water vibrations near TiO_2[21], alumina[22] and vapor[23] interfaces. It is, thus, of great interest to know if SCAN describes quantitatively the chemistry of water and, in particular, the thermodynamics and kinetics of water autoionization.

We calculated the PMF of water autoionization employing constrained MD, by selecting the distance of the OH bond from the dissociated water, hereafter referred to as O*-H*, as reaction coordinate (r_{OH}). We varied r_{OH} from 0.8 Å to 1.7 Å in increments of 0.05 Å. We then used semi-quantitative corrections for nuclear quantum effects (NQE) and long-range Coulomb interaction energy.

We obtained an absolute water pK_a that is only 1.0 pK_a unit different from the target value, i.e., in better agreement with experiments compared to results previously obtained with other functionals, such as BLYP[24-25]. First, we calculate the short-range interaction of water autoionization by looking at the PMF versus r_{OH} (Figure 1). Although previous simulations using the SCAN functional predicted an average length of water OH bonds is 0.98 Å[19], we find a relatively flat PMF (within error bars) between r_{OH} = 0.95 Å and 1.00 Å. When r_{OH} >= 1.7 Å, since the proton has been already transferred to H_3O^+, the major contribution to the free energy comes from the long-range interaction between OH^- and H_3O^+, which we modeled as a screened Coulomb interaction between two point charges. This allows us to compare the PMF at r_{OH} = 1.0 Å with that of the dissociated states, when OH^- and H_3O^+ are infinitely far apart. A direct

comparison of free energy between r_{OH} = 1.0 Å and 1.7 Å by SCAN (Figure 1) results in a free energy difference of 33.83 kT, where k is the Boltzmann constant and T is 300 K, corresponding to 14.69 pK_a units:

$$pK_a = \frac{|\Delta F|}{kT \times 2.3026} \qquad (3).$$

AIMD simulations describe how the water molecule becomes a OH^--H_3O^+ pair and to get the full pK_a of water, the free energy for the separation of such pair to infinity needs to be estimated as well. Here we use a crude approach by treating the ion pair as charges and by estimating their interaction using a coulombic form:

$$E_c = -\frac{1}{4\pi\epsilon_r\epsilon_0} \times \frac{e^2}{2.68} \times \frac{1}{10^{-20}kT} \qquad (4),$$

where ε_0 is the vacuum permittivity, ε_r is the relative permittivity of water (~78) and e is the elementary charge. The point charges located on the O* of OH^- and O_a of H_3O^+ atoms with charges -1e and +1e, respectively; we find that when O* and H* is constrained at 1.7 Å, the average distance between O* and O_a is 2.68 Å. We estimate the Coulomb contribution as the energy required to increase the distance between two opposite charges from 2.68 Å to infinity. The contribution from Coulomb interactions is 3.0 kT, corresponding to 1.3 pK_a units. We note that using a MS-EVB type model, the free energy for separating an amino acid anion from the hydronium moiety is about 2 kcal/mol,[26] corresponding to 1.5 pK_a units, i.e. comparable to our estimations.

To select the correct reference value we have to take into consideration NQEs. Markland and coworkers use the pK_a of D_2O and T_2O, to estimate the pH of classical water (i.e with nuclei of infinite-mass).[27] According to the estimate, the pH is 1.5 units higher than the canonical pH=7 value, corresponding to an increase of 3 units of the pK_a.[27] The following reaction is used to calculate the pKa:

$$HA(aq) + H_2O(l) \leftrightarrow A^-(aq) + H_3O^+(aq), \quad (5)$$

$$pKa = -log\frac{a(H^+)a(A^-)}{a(HA)a(H_2O)}. \quad (6)$$

It is important to remind the reader that the value 15.7, reported in many textbooks, comes from the incorrect assumption that a(HA) = [HA] = [H_2O] = 55 mol/L. The first problem with this identification between activity and concentration is that, while acceptable in the limit of infinite dilution, it is certainly not valid for a 55 M solution. More in detail, not all the water molecules can be identified as "reactants" since the vast majority of them are mere spectators to the reaction and thus should be considered "solvent" rather than "solute". In analogy with what is done for calculating the pK_a of any other acid, the activity of the solvent, $a(H_2O)$, should be assumed to be 1 (i.e. pure water, or, in other words, a large enough system that practically all the waters are available for hydrating solutes) and the activity of the reactive water, $a(HA)$, can be approximated with the analytic concentration at standard conditions (i.e. 1M). Only this definition of water pKa makes it homogeneous and therefore comparable with the pKa of other acids.[28] In our simulations, only 1 water is allowed to dissociate (which should be treated as solute) and other 54 water molecules are "solvent", corresponding to the 1 M concentration. With these assumptions, we take as a reference the pK_a value of 14.[28] As a result, with the 3 pK_a units from NQEs, target pK_a value is chosen as 17.

Notably, our calculations, including short-range and long-range interaction of the H^+-OH^- pair, predict a pK_a for water of 16.0, i.e. 1.0 pK_a unit lower than the target value. The difference is likely due to the imperfect definition of the reaction coordinate and the oversimplified model accounting for long-range Coulomb interactions. Nevertheless, when compared with the predictions from other functionals, namely BLYP[24-25] and HCTH[8], SCAN gives the best agreement and shows significant improvement over previous computational estimates. The PMF

contribution of water dissociation by BLYP-D3 is 14.36 pK_a units, 0.33 pK_a units lower than that of SCAN. Albeit modest, this improved description of the chemistry of water suggests that SCAN is a promising tool to study chemical reactions, the breaking and forming of covalent bonds. We carried out additional simulations using the coordination number as the collective variable[29-33] and obtained quantitatively consistent results (Figure. S1); this further confirms SCAN's accuracy in predicting the water pK_a.

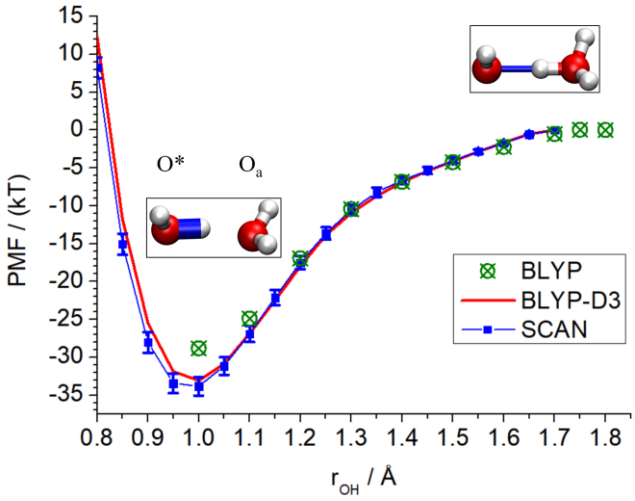

Figure 1. PMF of water autoionization. Results of "BLYP-D3" and "SCAN" are calculated in this work and "BLYP" is previous results.[24-25] The insets show the molecular structures of the reactants (r_{OH} = 1.0 Å) and products states (r_{OH} = 1.7 Å for SCAN and BLYP-D3). The free energy of the products state is set to 0. The blue cylinder in the molecular structures highlights the O*-H* bond kept constrained.

We also analyze how the proton H* leaves the water to reveal the mechanism of water autoionization. First, we compare the coordination number of the two water oxygens involved in the reaction as a function of the reaction coordinate r_{OH} (Figure 2). Here, the "rigid coordination number" is defined by assuming that each hydrogen atom belongs to its nearest oxygen.[24] Both simulations (based on SCAN or BLYP-D3) predict the following stages: 1) 1.0 Å < r_{OH} < 1.25 Å,

in this region, both waters have a coordination number of 2, indicating that the O*-H* covalent bond has not yet started to break yet; 2) 1.25 Å < r_{OH} < 1.35 Å, the coordination numbers of O* and O_a changes abruptly to 1 and 3, respectively, indicating that the proton transfer has happened and, in place of the two neutral water molecules, a OH^--H_3O^+ pair appears; 3) r_{OH} > 1.4 Å, the proton is completely transferred to O_a and, as r_{OH} keeps increasing, a positive-negative charge-pair is created that persist up to r_{OH}=1.7 Å. Beyond r_{OH} = 1.7 Å, proton transfer events will shuttle the excess proton away from the original pair, transforming the OH^--H_3O^+ into a water-water pair. It is worth mentioning that, in the limited time span of our simulations, when the OH^--H_3O^+ pair forms, the coordination number of OH^- is constantly 1 (exception for r_{OH} = 1.7 Å), indicating that no proton transfer on OH^- is observed; however, from r_{OH} > 1.55 Å, the coordination number of O_a is slightly lower than 3, due to proton transfer events from the hydronium ion to neighboring waters. Visual inspection of the trajectory at r_{OH} = 1.55 Å and 1.6 Å shows that one proton dangles between O_a and an oxygen near it forming a Zundel cation, whenever it lies in the middle of the two oxygens. However, the Zundel ion is only observed in a small fraction of all the configurations, consistent with an average coordination number very close to 3. The fact that proton transfer events involve more frequently hydronium than hydroxide ions is consistent with recent independent computational work.[16]

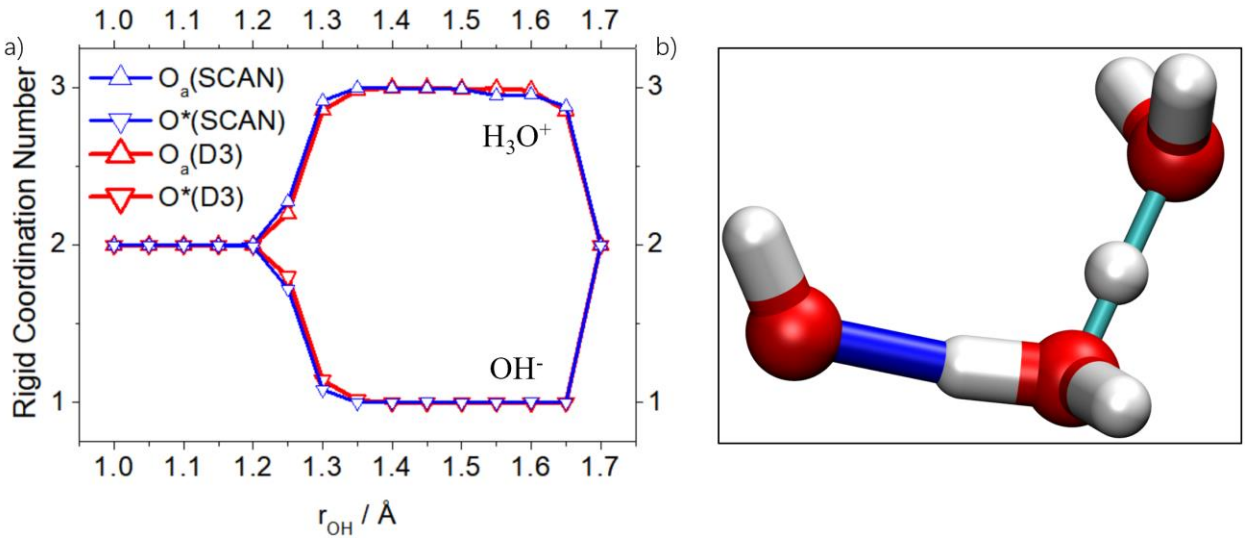

Figure 2. a) Average coordination number of O* and O_a as a function of the proton transfer reaction coordinate. Coordination numbers of 1 and 3 correspond to OH^- and H_3O^+, respectively. b) A molecular configuration from a simulation at r_{OH}=1.65 Å, in which the extra proton forms a Zundel ion. The blue line highlights the constrained O*-H* bond, while the cyan one indicates that the distance between O_a and its nearest oxygen is less than 2.43 Å, one of the hallmarks of the Zundel ion.[34]

The geometry of the OH^--H_3O^+ pair can be used to describe the process of water autoionization as well. As H* unbinds from O*, the H*-O_a distance decreases, indicating that as the O*-H* bond becomes weaker, the interaction between H* and O_a becomes stronger. When $r_{OH} \approx 1.3$ Å, $r_{OH} = r_{H*Oa} = 1/2 \times r_{O*Oa}$, the H* lies the middle between two oxygens. At $r_{OH} = 1.4$ Å, the O*-O_a distance reaches the global minimum (Figure 3); from here, the proton transfer has occurred and charges start to separate, consistent with the results of coordination numbers. The profile of the constraint force (Figure 4) also confirms this picture: it reaches the global minimum at r_{OH}=1.15 Å, which corresponds to an inflection point of the PMF. Past this point, the PMF starts to deviate significantly from a harmonic well and the "bond" between O* and H* starts to be

weaken. From r_{OH} =1.4 Å, the constraint force is approximately constant at a small negative value until r_{OH} = 1.7 Å, the largest distance explored in our simulations. The evolution of the coordination number, the geometry structure and constraint force predict one same fact that the O*-H* bond break begins at r_{OH} = 1.2 Å and is finally broken at r_{OH}=1.4 Å.

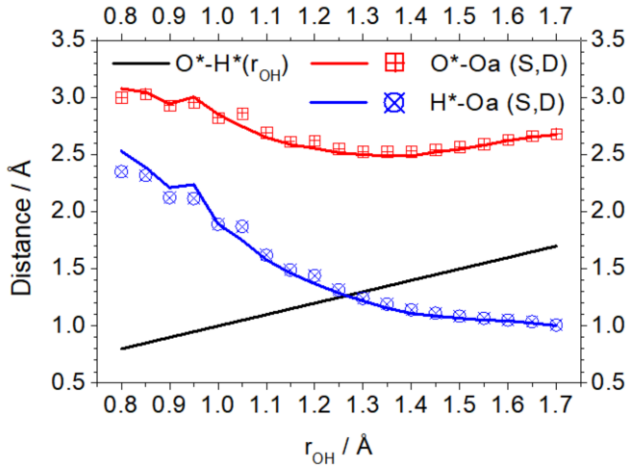

Figure 3. Average bond length of O*-O_a and H*-O_a with respect to r_{OH}. Red and blue lines are the results from SCAN simulations (marked as "S"), the square and circle symbols are the results from BLYP-D3 simulations (marked as "D"). The black curve is r_{OH}, as well as the distance of O*-H*.

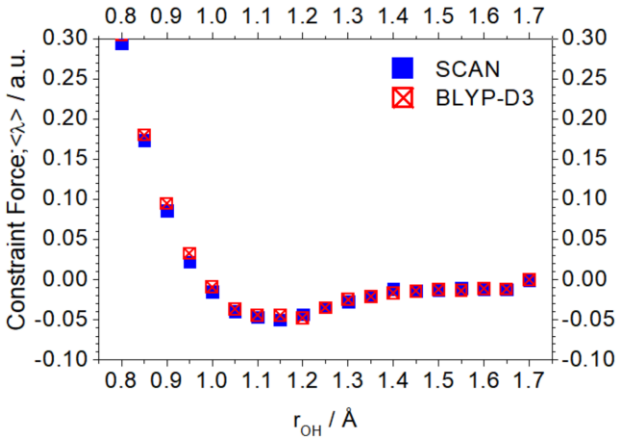

Figure 4. Average constraint force (in atomic units) for each window.

The radial distribution functions (RDFs) also show how different functionals affects the PMF of water autoionization. We compared $g_{OO}(r)$, $g_{OH}(r)$ and $g_{HH}(r)$ together with the distribution of the tetrahedral order parameter (as defined in ref. 35) from simulations based on SCAN, BLYP and BLYP-D3 (Figure 5). These are calculated on the constrained MD simulations trajectories at r_{OH} = 1.0 Å (the initial state). For the three RDFs, the results from SCAN are similar to those from BLYP-D3. Since our simulations are carried out at 300 K (and not at 330K as it is customary to mimic NQEs), we did observe an over-structured first shell and, consequently, more pronounced peaks and minima compared to experiments.[36] Relatively speaking, SCAN and BLYP-D3 predict a less ordered water structure compared to BLYP as apparent from both the $g_{OO}(r)$ and tetrahedral order parameter distribution (Figure 6). It is worth mentioning that the water OH bond length predicted by SCAN is slightly shorter than the BLYP one (Figure 5d), which may be one of the reasons why BLYP underestimates the water pK_a and overestimates the strength of the hydrogen bond network. We believed that correct RDFs, and more in general the structure of the first solvation shell, are essential to reproduce the correct chemical bond energy.

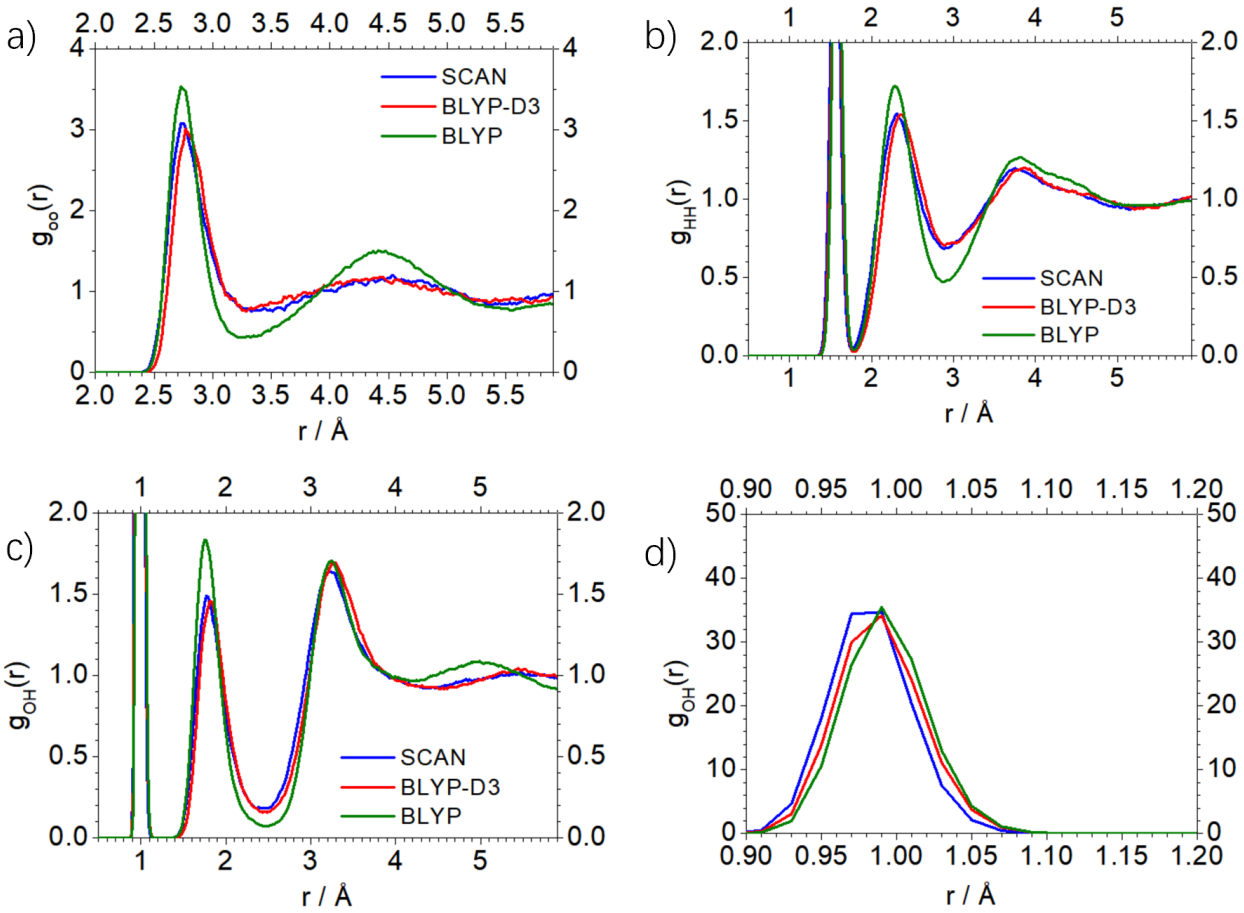

Figure 5. Radial distribution function. (a), (b) and (c) are $g_{OO}(r)$, $g_{HH}(r)$, $g_{OH}(r)$, respectively. (d) Close up of the first peak of $g_{OH}(r)$ showing the distribution of water OH bond length. Note that that the water OH bond length follows this series: $|OH|_{SCAN}<|OH|_{BLYP\text{-}D3}<|OH|_{BLYP}$.

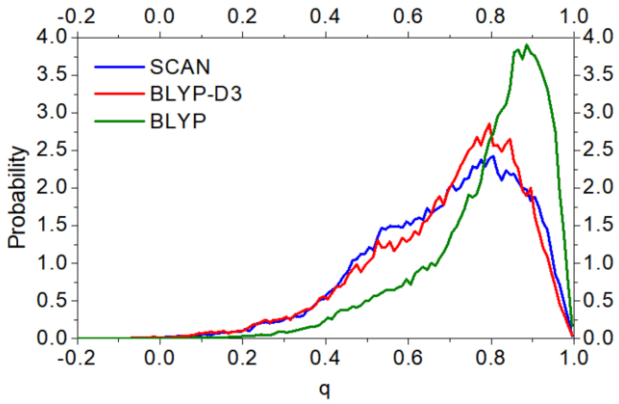

Figure 6. Tetrahedral order parameter probability distribution function. Trajectories used for this calculation are simulations in which r_{OH} is constrained at 1.0 Å.

This work also shows that BLYP-D3 predicts a similar free energy for water autoionization and water structures of bulk water. However, a recent paper by Yuki and coworkers shows that BLYP-D3 fails to predict water free-OH vibration at water/air interfaces[23]; in addition, the accuracy of BLYP for metals is questionable.[37] These issues limit BLYP's application to solid/water interfaces for which SCAN shows good results.[21-22] Having established that SCAN reproduces well the energetics of water dissociation, our results might be of crucial relevance for researchers working in related fields, such as water splitting near solid/water interfaces or calculation of pK_a of OH groups on mineral surfaces.

In conclusion, using AIMD and, in particular, CPMD, we calculated the PMF of water autoionization with the recently developed density functional SCAN; we used constrained MD and selected the O*-H* distance as reaction coordinate. From the PMF, we estimated the short-range contribution to the free energy of water autoionization, which turned out to be 33.8 kT, corresponding to 14.69 pK_a units. We then estimated the long-range Coulomb interactions to account for 3.0 kT, making the total pK_a of water 16.0, 1.0 pK_a unit lower than 17, the estimated target value for a perfect water model devoid of quantum effects.[27] This work shows that SCAN outperforms other functionals such as BLYP in describing the chemical reaction of water dissociation. While the addition of an empirical VDW correction (BLYP-D3) constitutes an improvement, the results based on SCAN are the closest to the target value. The approach used in this work can be easily applied to similar protonation/deprotonation reactions and our results constitute a reference for calculating the relative pK_a of small organic molecules or minerals at aqueous interfaces. Since this work demonstrates that SCAN functional successfully describes

the chemistry of water OH bond breaking, it is expected a good performance also for other chemical reactions, in particular for the prediction of free energy barriers and transition states in aqueous environment.

ASSOCIATED CONTENT

Supporting Information.

The following files are available free of charge.

Simulation details, including those using OH distance or smoothed coordination number as collective variables, further comparison of these two CVs. (PDF)

AUTHOR INFORMATION

Corresponding Authors

*(E.B.) E-mail:eborguet@temple.edu.

*(V.C.) E-mail:vincenzo.carnevale@temple.edu

Notes

The authors declare no competing financial interests.

ACKNOWLEDGEMENTS

This work was supported as part of the Center for Complex Materials from First Principles (CCM), an Energy Frontier Research Center funded by the U.S. Department of Energy, Office of Science, Basic Energy Sciences under Award #DE-SC0012575. This research includes calculations carried out on Temple University's HPC resources and thus was supported in part by the National Science Foundation through major research instrumentation grant number 1625061

and by the US Army Research Laboratory under contract number W911NF-16-2-0189. R.W. thanks Temple University for the support of a Presidential Fellowship.

REFERENCES

1. Agmon, N.; Bakker, H. J.; Campen, R. K.; Henchman, R. H.; Pohl, P.; Roke, S.; Thämer, M.; Hassanali, A., Protons and Hydroxide Ions in Aqueous Systems. *Chem. Rev.* **2016**, *116*, 7642-7672.

2. Jencks, W. P., General Acid-Base Catalysis of Complex Reactions in Water. *Chem. Rev.* **1972**, *72*, 705-718.

3. Chen, Y.-L.; Doltsinis, N. L.; Hider, R. C.; Barlow, D. J., Prediction of Absolute Hydroxyl Pka Values for 3-Hydroxypyridin-4-Ones. *J. Phys. Chem. Lett.* **2012**, *3*, 2980-2985.

4. Wang, R.; DelloStritto, M.; Remsing, R. C.; Carnevale, V.; Klein, M. L.; Borguet, E., Sodium Halide Adsorption and Water Structure at the α-Alumina(0001)/Water Interface. *J. Phys. Chem. C* **2019**, *123*, 15618-15628.

5. Carnevale, V.; Fiorin, G.; Levine, B. G.; DeGrado, W. F.; Klein, M. L., Multiple Proton Confinement in the M2 Channel from the Influenza a Virus. *J. Phys. Chem. C* **2010**, *114*, 20856-20863.

6. Liang, R.; Li, H.; Swanson, J. M. J.; Voth, G. A., Multiscale Simulation Reveals a Multifaceted Mechanism of Proton Permeation through the Influenza a M2 Proton Channel. *PNAS* **2014**, *111*, 9396.

7. Ivanov, I.; Klein, M. L., Deprotonation of a Histidine Residue in Aqueous Solution Using Constrained Ab Initio Molecular Dynamics. *J. Am. Chem. Soc.* **2002**, *124*, 13380-13381.

8. Ivanov, I.; Chen, B.; Raugei, S.; Klein, M. L., Relative pK_a Values from First-Principles Molecular Dynamics: The Case of Histidine Deprotonation. *J. Phys. Chem. B* **2006**, *110*, 6365-6371.

9. Bankura, A.; Klein, M. L.; Carnevale, V., Proton Affinity of the Histidine-Tryptophan Cluster Motif from the Influenza a Virus from Ab Initio Molecular Dynamics. *Chem. Phys.* **2013**, *422*, 156-164.

10. Leung, K.; Nielsen, I. M. B.; Criscenti, L. J., Elucidating the Bimodal Acid−Base Behavior of the Water−Silica Interface from First Principles. *J. Am. Chem. Soc.* **2009**, *131*, 18358-18365.

11. Pfeiffer-Laplaud, M.; Costa, D.; Tielens, F.; Gaigeot, M. P.; Sulpizi, M., Bimodal Acidity at the Amorphous Silica/Water Interface. *J. Phys. Chem. C* **2015**, *119*, 27354-27362.

12. Sulpizi, M.; Sprik, M., Acidity Constants from Vertical Energy Gaps: Density Functional Theory Based Molecular Dynamics Implementation. *PCCP* **2008**, *10*, 5238-5249.

13. Parashar, S.; Lesnicki, D.; Sulpizi, M., Increased Acid Dissociation at the Quartz/Water Interface. *J. Phys. Chem. Lett.* **2018**, *9*, 2186-2189.

14. Park, J. M.; Laio, A.; Iannuzzi, M.; Parrinello, M., Dissociation Mechanism of Acetic Acid in Water. *J. Am. Chem. Soc.* **2006**, *128*, 11318-11319.

15. Chen, M.; Ko, H.-Y.; Remsing, R. C.; Calegari Andrade, M. F.; Santra, B.; Sun, Z.; Selloni, A.; Car, R.; Klein, M. L.; Perdew, J. P., et al.,, Ab Initio Theory and Modeling of Water. *PNAS* **2017**.

16. Chen, M.; Zheng, L.; Santra, B.; Ko, H.-Y.; DiStasio Jr, R. A.; Klein, M. L.; Car, R.; Wu, X., Hydroxide Diffuses Slower Than Hydronium in Water Because Its Solvated Structure Inhibits Correlated Proton Transfer. *Nat. Chem.* **2018**, *10*, 413-419.

17. Sun, J.; Ruzsinszky, A.; Perdew, J. P., Strongly Constrained and Appropriately Normed Semilocal Density Functional. *Phys. Rev. Lett.* **2015**, *115*, 036402.

18. Sun, J.; Remsing, R. C.; Zhang, Y.; Sun, Z.; Ruzsinszky, A.; Peng, H.; Yang, Z.; Paul, A.; Waghmare, U.; Wu, X., et al., Accurate First-Principles Structures and Energies of Diversely Bonded Systems from an Efficient Density Functional. *Nat. Chem.* **2016**, *8*, 831.

19. Zheng, L.; Chen, M.; Sun, Z.; Ko, H.-Y.; Santra, B.; Dhuvad, P.; Wu, X., Structural, Electronic, and Dynamical Properties of Liquid Water by Ab Initio Molecular Dynamics Based on Scan Functional within the Canonical Ensemble. *J. Chem. Phys.* **2018**, *148*, 164505.

20. Xu, J.; Chen, M.; Zhang, C.; Wu, X., First-principles Study of the Infrared Spectrum in Liquid Water from a Systematically Improved Description of H-bond Network. *Phys. Rev. B* **2019**, *99*, 205123.

21. Calegari Andrade, M. F.; Ko, H.-Y.; Car, R.; Selloni, A., Structure, Polarization, and Sum Frequency Generation Spectrum of Interfacial Water on Anatase TiO_2. *J. Phys. Chem. Lett.* **2018**, *9*, 6716-6721.

22. DelloStritto, M. J.; Piontek, S. M.; Klein, M. L.; Borguet, E., Effect of Functional and Electron Correlation on the Structure and Spectroscopy of the $Al_2O_3(001)$–H_2O Interface. *J. Phys. Chem. Lett.* **2019**, *10*, 2031-2036.

23. Ohto, T.; Dodia, M.; Xu, J.; Imoto, S.; Tang, F.; Zysk, F.; Kühne, T. D.; Shigeta, Y.; Bonn, M.; Wu, X., et al., Accessing the Accuracy of Density Functional Theory through Structure and Dynamics of the Water–Air Interface. *J. Phys. Chem. Lett.* **2019**, *10*, 4914-4919.

24. Trout, B. L.; Parrinello, M., Analysis of the Dissociation of H_2O in Water Using First-Principles Molecular Dynamics. *J. Phys. Chem. B* **1999**, *103*, 7340-7345.

25. Trout, B. L.; Parrinello, M., The Dissociation Mechanism of H_2O in Water Studied by First-Principles Molecular Dynamics. *Chem. Phys. Lett.* **1998**, *288*, 343-347.

26. Nelson, J. G.; Peng, Y.; Silverstein, D. W.; Swanson, J. M. J., Multiscale Reactive Molecular Dynamics for Absolute pKa Predictions and Amino Acid Deprotonation. *J. Chem. Theory Comput.* **2014**, *10*, 2729-2737.

27. Ceriotti, M.; Fang, W.; Kusalik, P. G.; McKenzie, R. H.; Michaelides, A.; Morales, M. A.; Markland, T. E., Nuclear Quantum Effects in Water and Aqueous Systems: Experiment, Theory, and Current Challenges. *Chem. Rev.* **2016**, *116*, 7529-7550.

28. Silverstein, T. P.; Heller, S. T., p K a Values in the Undergraduate Curriculum: What Is the Real pKa of Water? *J. Chem. Educ.* **2017**, *94*, 690-695.

29. Davies, J. E.; Doltsinis, N. L.; Kirby, A. J.; Roussev, C. D.; Sprik, M., Estimating pKa Values for Pentaoxyphosphoranes. *J. Am. Chem. Soc.* **2002**, *124*, 6594-6599.

30. Doltsinis, N. L.; Sprik, M., Theoretical pKa Estimates for Solvated $P(OH)_5$ from Coordination Constrained Car–Parrinello Molecular Dynamics. *PCCP* **2003**, *5*, 2612-2618.

31. Sandmann, N.; Bachmann, J.; Hepp, A.; Doltsinis, N. L.; Müller, J., Copper(II)-mediated Base Pairing Involving the Artificial Nucleobase 3H-imidazo[4,5-f]quinolin-5-ol. *Dalton Trans.* **2019**, *48*, 10505-10515.

32. Sprik, M., Coordination Numbers as Reaction Coordinates in Constrained Molecular Dynamics. *Faraday Discuss.* **1998**, *110*, 437-445.

33. Sprik, M., Computation of the pK of Liquid Water Using Coordination Constraints. *Chem. Phys.* **2000**, *258*, 139-150.

34. Stoyanov, E. S.; Stoyanova, I. V.; Reed, C. A., The Structure of the Hydrogen Ion (H_{aq}^{+}) in Water. *J. Am. Chem. Soc.* **2010**, *132*, 1484-1485.

35. Errington, J. R.; Debenedetti, P. G., Relationship between Structural Order and the Anomalies of Liquid Water. *Nature* **2001**, *409*, 318.

36. Skinner, L. B.; Huang, C.; Schlesinger, D.; Pettersson, L. G. M.; Nilsson, A.; Benmore, C. J., Benchmark Oxygen-Oxygen Pair-Distribution Function of Ambient Water from X-Ray Diffraction Measurements with a Wide Q-Range. **2013**, *138*, 074506.